Concentration measurement of injected gaseous fuel using quantitative schlieren and optical tomography

Emishaw D. Iffa
emishawd@gmail.com
Center for Automotive Research, Universiti Teknologi PETRONAS, Block N, 31750 Tronoh, Perak, Malaysia

A. Rashid A. Aziz
rashid@petronas.com.my
Center for Automotive Research, Universiti Teknologi PETRONAS, Block N, 31750 Tronoh, Perak, Malaysia

Aamir S. Malik
aamir_saeed@petronas.com.my
Department of Electrical and Electronic Engineering, Universiti Teknologi PETRONAS, 31750 Tronoh, Perak, Malaysia

In this paper, the quantitative schlieren method is extended to measure the concentration field of an injected gaseous fuel along several planes perpendicular to the jet axis. Background Oriented Schlieren (BOS) is used as a quantitative flow field concentration measurement based on the deflection made by features in the background pattern. The flow field which is located between the camera and the background pattern changes the intensity value of the background points in the transfer medium. The optical flow algorithm, which is used to measure the deflection vectors in the background due to the change in index of refraction, is modified to consider the change in intensity of the background image due to the flow field. Optical tomography is used as a tool to extract the index of refraction of the gaseous field. Mole fraction values at different planes perpendicular to the jet axis are obtained and displayed. [DOI: 10.2971/jeos.2010.10029]

Keywords: background oriented schlieren, index of refraction, mole fraction, optical flow, optical measurements, optical tomography

1 INTRODUCTION

The limitations of world's fossil fuel supply and the ever increasing stringent pollution policies have brought an extensive research focus on alternative fuels. Alternative fuels like natural gas are believed to reduce pollutant emission from vehicles and power plants [1].

In order to get an improved combustion and minimize NOX emission, the air fuel mixture needs to be controlled and fuel distribution measurements are necessary to improve the mixing process. Unlike liquid fuel, the compressed natural gas jet has variable density flow due to its high expansion and a thin outer boundary layer [1, 2].

To measure the gas density distribution, intrusive and non-intrusive types of measurements can be used. Using non-intrusive techniques has advantages since they do not perturb the flow. The most commonly used optical gas flow visualization techniques for measuring density (concentration) distribution use the basic principles of electron beam fluorescent images, scattered light images or light deflection [3, 4].

The intensity of fluorescent emission due to excitation of atoms or molecules of a gas that is intercepted by an electron sheet is proportional to the local number density. These electron beam measurements are usually used to measure density values of specific spatial points [3].

Light scattering that involved either elastic (non-energy exchanging) or inelastic (energy-exchanging) scattering processes from atoms or molecules can be used as quantitative measurement of compressible turbulent flow measurement [4]. These techniques are usually used without seeding flows so as not to perturb the concentration distribution within the flow. Since there is no seeding in the flow, the signal obtained by Rayleigh scattering technique is weak and needs to be intensified.

Schlieren technique, on the other hand, is a method that uses the deflection of light due to the change in field density to visualize the density gradients in gas flow [5]. It is most commonly used for qualitative investigations. To employ this technique as a quantitative measurement tool, a certain calibration has to be employed [6]. Background oriented schlieren (BOS) is one of the quantitative measurement methods that makes use of the distorted background image due to changes in the transfer medium. It was first reported by Dalziel [7] as a qualitative density fluctuation measurement.

Venkatakrishnan and Meier [8] have developed a 3-dimensional density distribution of an air jet by using computed tomography. They computed the index of refraction as a line integral and developed a 3-dimensional density field based on filtered back projection algorithm

Goldhahn and Seume [9] considering projections taken with BOS as gradient information, have shown the possibility of directly employing a computed tomography to the deflection measurement of BOS. Leopold has attempted to apply a color background pattern in order to increase the BOS system resolution [10].

Received 16 January, 2010; published 22 June, 2010 ISSN 1990-2573

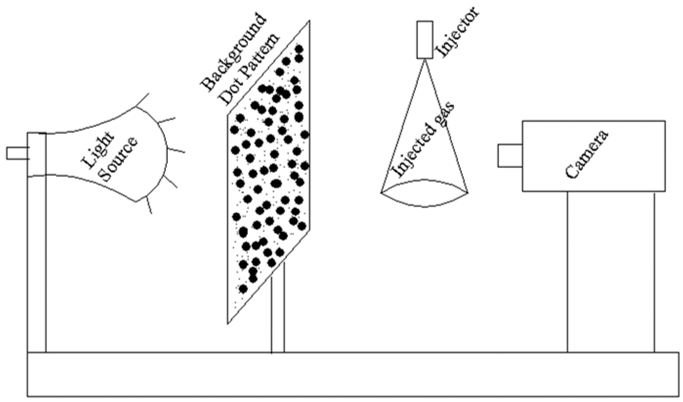

FIG. 1 BOS set-up.

The background pattern displacement can be measured by optical flow algorithms. Most of BOS publications make use of Particle Image Velocimetry (PIV) like window based cross correlation algorithms for measuring the background feature displacement. Atcheson *et al.* [11] compares different optical flow algorithms to compute the displacement vectors of the dot pattern. They also propose a multiscale background pattern to avoid different tedious reprint of the background pattern for the appropriate experimental configuration and helps to accurately down sample the images in order to handle large displacements without the loss of accuracy [11, 12].

This paper utilizes a background oriented schilieren method to quantitatively visualize the whole concentration field distribution of near nozzle injected CNG fuel. The wavelet noise is used to generate the background pattern and background displacements are found using Lucas-Kanade optical flow algorithm. Computed Tomography is implemented to determine the concentration fields along the radial axis.

2 MEASUREMENT PRINCIPLES AND METHODOLOGY

BOS works based on evaluation of image variations due to change in refractive index of the propagation medium. An image is a convolution between its target object and the transfer channel. A change in one of these two parameters changes the image captured by the sensor. BOS exploits this advantage by comparing images with normal and disturbed transfer channel.

A camera, as shown in Figure 1, is focused on the background pattern. It captures two kinds of images; one with the density field to be studied while the other one without the flow field.

Correlating the two images gives the background pattern displacement vector. The light beam deflection equation, Eq. (1), relates the displacement vectors with the field gradient index of refraction field, through which the light beam passes.

By taking paraxial approximation and small deflection angles into account, the Cartesian components of the light deflection angle due to change in density field can be found using geometrical optics principle. Eq. (1) shows the integration of geometrical optics ray equation

$$\varepsilon_x(x,y) = \int_l \frac{1}{n}\frac{\partial n(x,y)}{\partial x} dz$$
$$\varepsilon_y(x,y) = \int_l \frac{1}{n}\frac{\partial n(x,y)}{\partial y} dz \qquad (1)$$

where ε is the light deflection angles in x,y directions and n is index of refraction.

The index of refraction and density field are linearly related by Gladstone-Dale equation

$$n - 1 = G(\lambda)\rho \qquad (2)$$

where $G(\lambda)$ is Gladstone-Dale constant and ρ is density of the test field.

The fuel injection system parameters are shown in Table 1. The CNG-fuel injection system is modified to obtain a continuous solid cone gaseous fuel injection and a constant volume chamber with provision for optical access are constructed as the main components of the fuel injection system. Fuel exit pressures are varied from 250 KPA to 1 MPA. The injector nozzle has constant 2 mm hole diameter.

Injection Parameters	Type/Amount
Fuel	CNG
Injection Pressure	0.25 MPA to 1 MPA
Injection Temperature	200°C
Downstream Pressure	0.1007 MPA
Downstream Temperature	27.1°C
Injector Nozzle diameter	2 mm

TABLE 1 Fuel injection parameters.

The optical measurement (BOS) set-up consists of a wavelet noise generated background pattern, optical lenses, Xenon stroboscope light, Photron Fastcam-x 1280 PCL high speed camera with Nikkor optical lens of 60 mm focal length and Fastcam Control software. A wavelet noise developed by Cook and DeRose [13] is generated and printed on transparency using a laser jet printer.

The distance between the background pattern and the center of the nozzle was 1112.11 mm whereas; the distance between the camera lens and the center of the nozzle was 583.14 mm. Having a larger distance between the background pattern and the density field than the distance between the camera and the density field increases the system sensitivity [9]. The resolution of the camera and the shutter time used were 1280×1024 and $1/1000$ s respectively.

3 BOS IMAGE PROCESSING

The displacement vectors of the background pattern can be computed using PIV like window based interrogation technique or other optical flow algorithms. The former practice is the most widely used technique in BOS experiments. The optical flow algorithms use local derivatives to approximate the image motion of optical interest. In our case it is the displacement of the background feature. Optical flow assumes that all the temporal intensity change between two images are due to motion of the object only. Recent studies have shown that the gradient based optical flow algorithms suit BOS technique better than block matching algorithms since an image intensity (I) is the convolution of the object function (O) and transfer function (T) [11].

$$I = B * T\,. \tag{3}$$

It is obvious that the change in transfer medium affects the background image intensity. This paper uses a modified optical flow algorithm that takes into account intensity variation. Based on the light beam deflection, filtered back projection is used to reconstruct two dimensional index of refraction information. Once the index of refraction is obtained, the gas concentration can be computed by Gladstone–Dale equation of gas mixtures. The following sub-sections show the mathematical model used to measure the fuel concentration.

3.1 Light beam deflection measurement

In PIV data, the flow and the tracer particles both exist in the pair of frames to be correlated. This trend indicates that there won't be a significant intensity variation in PIV images and if there is, then it could be easily corrected using post image processing methods. On the other hand, the pair of BOS images used for correlation are taken with and without the flow field. This situation creates a significant intensity variation that demands consideration. We have addressed this problem by modifying the flow equation.

The 2D motion constraint equation states that a pixel with intensity $I(x,y,t)$ moves by δx and δy in time δt to $I(x+\delta x, y+\delta y, t+\delta t)$. In BOS this happens due to the variable index of refraction of the jet flow in between the camera and the background pattern. The 2D motion constraint equation can be stated as Eq. (4) [14]

$$\frac{\partial I}{\partial x}\delta x + \frac{\partial I}{\partial y}\delta y + \frac{\partial I}{\partial t}\delta t = 0 \tag{4}$$

where δt is taken to be unity for ease of calculation. Therefore, Eq. (4) is the optical flow differential equation which assumes that object points maintain their intensity values.

Previous literature has shown that most of the deflectionvector computing techniques are either region based (PIV like) algorithms [8]–[10] or techniques which use first order differential techniques [11]. Both techniques assume constant pixel intensity. However, this assumption only works when there are no changes in illumination and camera lens distortion as well as no change for many other factors that affect the assumed image intensity invariance.

Suppose $I(x+\delta x, y+\delta y, t+\delta t)$ is the background pixel intensity during injection. Same background point $I(x,y,t)$ without injection can be multiplied by a certain pixel constant k to account for pixel intensity change. Based on Taylor series $I(x+\delta x, y+\delta y, t+\delta t)$ can be written in the form of

$$\begin{aligned} & I(x+\delta x, y+\delta y, t+\delta t) \\ & = I(x,y,t) + \frac{\partial I}{\partial x}\delta x + \frac{\partial I}{\partial y}\delta y + \frac{\partial I}{\partial t}\delta t + H.O.T. \\ & = kI(x,y,t)\,. \end{aligned} \tag{5}$$

Truncating Higher Order Terms ($H.O.T$) and using the intensity value before injection the following equation is obtained

$$(k-1)I(x,y,t) = \frac{\partial I}{\partial x}\delta x + \frac{\partial I}{\partial y}\delta y + \frac{\partial I}{\partial t}\delta t \tag{6}$$

δt is the time difference between two frames and can be taken as $1/\text{fps}$ (fps stands for frame per second). The spatial intensity derivatives $\partial I/\partial x$ and $\partial I/\partial y$ and the temporal intensity derivative $\partial I/\partial t$ can be directly computed using finite difference method. This leaves Eq. (6) with three unknowns δx, δy and k. To solve for these unknowns, a system like Lucas-Kande first order differential is used [14].

The principle of Lucas-Kanade is to mitigate 'the aperture problem' by employing a technique that minimizes the residual function f using the least square minimization method in order to solve the over determined equations and provide the required motion vectors. It fits the required displacement from estimates of the local neighborhood pixels [14]

$$f(d) = \sum_{U-P}^{U+P}\sum_{V-N}^{V+N}\left((k-1)I(x,y,t) - \left(\frac{\partial I}{\partial x}\delta x + \frac{\partial I}{\partial x}\delta y + \frac{\partial I}{\partial t}\delta t\right)\right)^2 \tag{7}$$

where U and V are the coordinates for the pixel of interest while P and N are positive integers. The image neighborhood will have a size of $(2P+1, 2N+1)$. Eq. (7) is modified by adding a 2D Gaussian weighting function to provide a higher weight to the central pixel.

The selected neighborhood window is 5×5 pixels. To increase the sensitivity and accuracy of the algorithm, pyramidal image representation and sub pixel approximation using bilinear interpolation is employed. The pyramidal representation helps to capture large pixel displacements than neighborhood window.

The displacement vectors are converted into angle of deflections based on the relative position of background pattern, camera lens and concentration field location within the BOS set-up.

3.2 Computed tomography

Tomography gives an ability to visualize the internal flow structure of a test object by reconstructing the image data taken from different projection angles. It is used to illustrate three dimensional concentration field of an injected jet from BOS displacement vector data. The image reconstruction principles from the concentration distribution measurement perspective are discussed below. The angle of deflection measured along s (see Figure 2) can be related to the index of refraction $n(r,s)$ along a plane perpendicular to the jet axis by Eq. (8) as

$$\varepsilon(\theta,s) = \frac{d}{ds}\int_l n'(r,s)dr \tag{8}$$

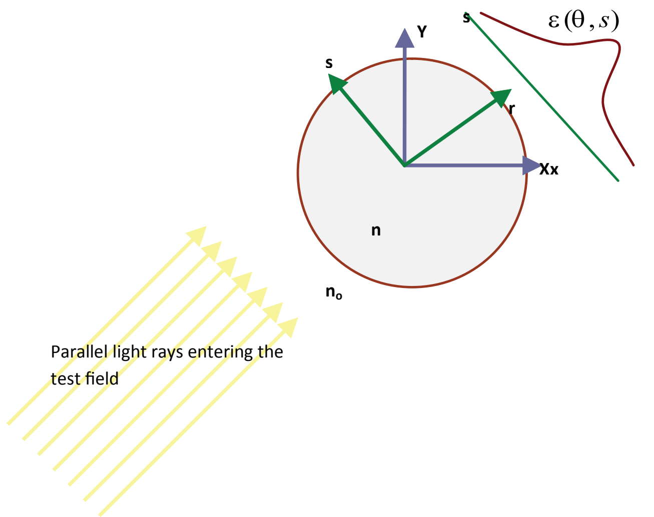

FIG. 2 The light rays deflection plane t and s.

where $n' = \frac{n(r,s)}{n_o}$, $n(r,s)$ and n_o are the indices of refraction of the injected gas in the plane r-s and the ambient index of refraction respectively.

The convolution of Eq. (8) with filter from [9] results in the following

$$n'(x,y) = \int_0^{\pi} \int_{-\infty}^{\infty} \frac{|w|}{i2\pi w} e^{i2\pi ws} \varepsilon(\theta,s) dw d\theta \tag{9}$$

The above equation gives the normalized index of refraction of the injected jet in a plane perpendicular to the jet axis. The density distribution in the same plane can be obtained using the Gladstone-Dale equation. The 3-dimensional density field is obtained by stacking up the above 2-dimensional density distribution slices.

By using the Gladstone-Dale equation for gas mixtures, the concentration measurements of the CNG fuel is evaluated as

$$n - 1 = \sum_i G_i(\lambda)\rho_i \tag{10}$$

where i is the species type.

Since natural gas is a stable gas under normal conditions, it is treated as a single gas. Thus the species available on the flow are CNG and air. Air is assumed to comprise of 21% oxygen and 79% nitrogen.

By using the ideal gas equation the concentration measurement of species mole fraction can be found using Eq. (10)

$$n - 1 = \frac{P}{RT} \sum_i G_i(\lambda) X_i M_i \tag{11}$$

where X_i is species mole fraction and M_i is species molecular weight.

4 RESULTS AND DISCUSSION

Verifying the experimental repeatability and measuring the accuracy of optical flow and tomographic algorithms are the two distinct steps used to validate the experimental and image processing procedures. The structural similarity index (SSIM) is used to show that the assumed steady state and the experimental repeatability are achieved within acceptable limits. Synthetic data evaluation is used to measure the performance of image processing tasks, which are the optical flow algorithm and optical tomography.

4.1 Data repeatability

Earlier experiments [15] have observed that oscillations appear at Reynolds number $(Re) > 160$, and the length to diameter of the nozzle ratio is $(L/D) > 7$ or $(Re - 100) \times L/D > 300$. Since the near nozzle air fuel mixture is the important parameter for improved combustion and to avoid self sustained oscillation, this paper studied near nozzle flow region at a Reynolds number much less than 160.

Both transient and steady oscillating flows have a tendency to give a dissimilar image contrast and luminosity for flow images taken at different temporal dimensions. In this study, the flow is imaged using both conventional schlieren and BOS techniques at a frame speed of 16000 frames per second. The intensity and contrast variation between images at different times are measured based on SSIM criteria. Wang *et al.* [16] has proposed SSIM as

$$SSIM = \frac{(2\mu_x\mu_y + C1)(2\sigma_{xy} + C2)}{(\mu_x^2 + \mu_y^2 + C1)(\sigma_x^2 + \sigma_y^2 + C2)} \tag{12}$$

where μ_x and μ_y are mean intensity images and σ_x and σ_y are standard deviations of images

$$\sigma_{xy} = \frac{1}{N-1} \sum_{i-1}^{N} (x_i - \mu_x)(y_i - \mu_i) \tag{13}$$

x_i and y_i are pixel intensities of image x and y.

Pairs of images are randomly selected from database of BOS and conventional schlieren images. The similarities between random pair of images are computed using SSIM. The mean value of SSIM is found to be 0.9794 and 0.9664 for BOS and conventional schlieren images respectively (where unity is a value for identical images). This result gives a provision to assume the flow under study is a steady nonoscillating flow. The SSIM value also confirms that the noise occurring due to vibration of the camera, background and fuel injector is within acceptable limit.

4.2 Accuracy of the algorithms

The accuracy of the BOS set up is measured using synthetic data evaluation. A known volumetric (density) field of injected fuel data from [17] is used as a variation of index of refraction test field in a virtual BOS optical setup. The virtual BOS setup was arranged using ray casting method. Rays start from virtual camera position passed through gasoline vapor volumetric information and struck the observation area. This area was represented by wavelet noise virtual background. The relative distance from the background and the volumetric data to the virtual imaging plane was 5:2. The accuracy potential was defined by a standard deviation of 0.1 pixels

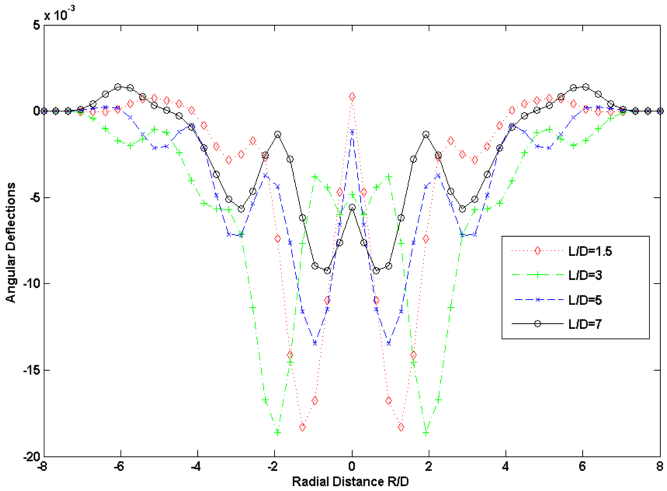

FIG. 3 Angular deflection vectors along radial axis.

in image plane. A similar imaginary setup excluding the volumetric data was used to capture the background image in order to simulate the background image without flow. These pair of images with and without the known volumetric density field were used as inputs to optical flow and tomography algorithms in order to calculate the index of refraction (density of the field). The density distribution obtained by the virtual BOS experiment is compared with the given density field and a RMS error of 1.17 is found. This RMS value gives confidence that a good accuracy is attained.

4.3 BOS results

The angular deflection vectors for different cross sectional planes along the radial axis are plotted in Figure 3. Power spectral density estimation is used to find out the cutoff frequency for filtering the angular deflection data. Based on the results from power spectral density estimation, a normalized frequency of 0.47 is selected to be the cutoff frequency and values higher than 0.47 are taken as noise and removed.

The normalized index of refraction, Eq. (9) is obtained using filtered back projection. Figure 4 shows the change in index of refraction of the test field from the ambient index of refraction at different planes perpendicular to the nozzle axis. To add visibility, the change in index of refraction is multiplied by 1000.

Figure 5 portrays the concentration of the CNG fuel in the near nozzle region. The figure also displays the fuel expansion area at different transverse planes. The fuel concentration is portrayed in terms of mole percentage.

5 CONCLUSION

This paper implemented the BOS technique to measure near nozzle gaseous fuel concentration. Gaseous fuel was injected in a constant volume chamber and the variation in index of refraction due to density distribution was captured and analyzed using optical flow algorithms. We implemented a modified Lucas-Kanade displacement vector computing method

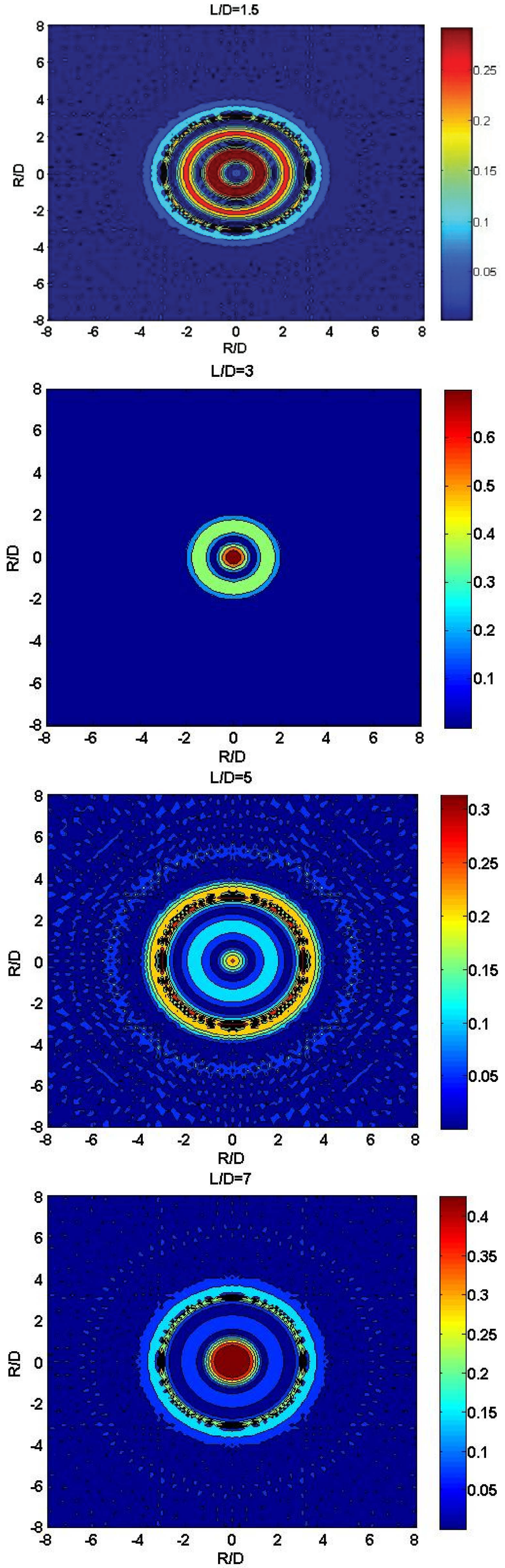

FIG. 4 Change in index of refraction at different planes perpendicular to the jet axis.

which accounts for the change in intensity of background due to the presence of a flow field The displacement fields ob-

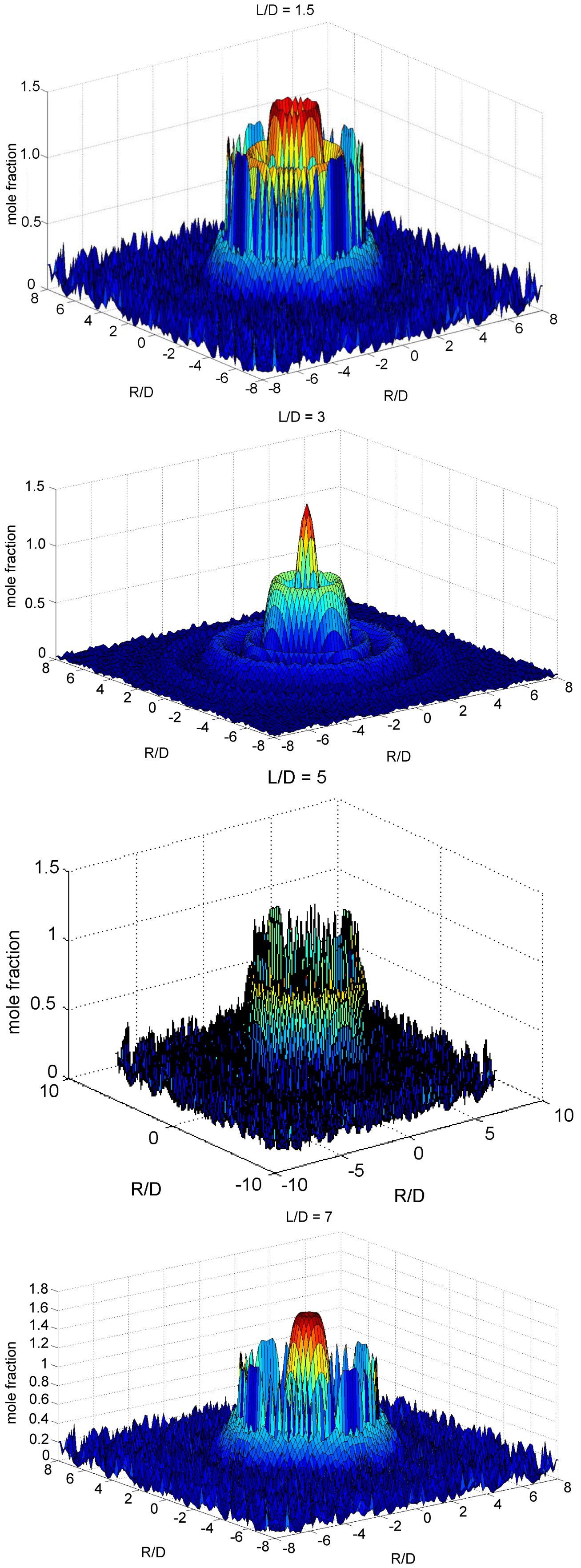

FIG. 5 Change in index of refraction at different planes perpendicular to the jet axis.

tained based on Lucas-Kanade optical flow algorithm were validated using synthetic data evaluation. The acquired deflection vector was adapted to index of refraction by means of geometrical optics equation and computed tomography. Gladstone-Dale equation for mixture of gases is used to determine the CNG fuel concentration. Various concentration values at different planes of the jet were computed and displayed.

References

[1] L. Ben, G. Charnay, R. Bazile, and B. Ferret, "Quantitative imaging of equivalence ratios in a natural gas SI engine flow bench using acetone fluorescence" Exp. Fluids **43**, 77–88 (2007).

[2] J. Abraham, V. Magi, J. Macinnes, and F. Bracco, *Gas versus spray injection: which mixes faster?* (SAE Technical Paper 940895, 1994).

[3] M. Belan, S. DePonte, and D. Tordella, "Determination of density and concentration from fluorescent Images of gas flow" Exp. Fluids **45**, 501–511 (2008).

[4] A. Milke, "Development of a molecular Rayleigh scattering diagnostic for simultaneous time-resolved measurement of temperature, velocity and density" (PhD Thesis, Case Western Reserve University, 2008).

[5] G. S. Settles, *Schlieren and Shadowgraph Techniques* (Springer-Verlag, Berlin, 2001).

[6] E. Elsinga, B. W. Oudheusden, F. Scarano, and D. W. Watt, "Assessment and application of quantitative schlieren methods: calibrated color schlieren and background oriented schlieren" Exp. Fluids **36**, 309–325 (2004).

[7] S. B. Dalziel, G. O. Hughes, and B. R. Sutherland, *Synthetic Schlieren* (8th International Symposium on Flow Visualization, Sorrento, 1–4 September 1998).

[8] L. Venkatakrishnan, and G. E. A. Meier, "Density measurements using the background oriented schlieren technique" Exp. Fluids **37**, 237–247 (2004).

[9] E. Goldhahn, and J. Seume, "Quantitative measurements of three-dimensional density fields using the background oriented schlieren technique" Exp. Fluids **43**, 241–249 (2007)

[10] F. Leopold, *The Application of the Colored Background Oriented Schlieren Technique (CBOS) to Free-Flight and In-Flight Measurements* (22nd International Congress on Instrumentation in Aerospace Simulation Facilities, Pacific Grove, 10–14 June 2007).

[11] B. Atcheson, W. Heidrich, and I. Ihrke, "An evaluation of optical flow algorithms for background oriented schlieren imaging" Exp. Fluids **46**, 467–476 (2009).

[12] B. Atcheson, I. Ihrke, B. Derek, W. Heidrich, M. Magnor, and H. P. Seidel, *Imaging and 3D Tomographic Reconstruction of Time Varying Inhomogeneous Refractive Index Fields* (24th International Conference and Exhibition on Computer Graphics and Interactive Techniques SIGGRAPH 2007, San Diego, 5–9 August 2007).

[13] R. Cook, and T. De Rose, "Wavelet noise" ACM T. Graphic **24**, 803–811 (2005).

[14] J. L. Barron, D. J. Fleet, and S. S. Beauchemin, "Performance of optical flow techniques" Int. J. Comput. Vision **12**, 43–77 (1994).

[15] A. Maurel, P. Ern, B. J. A. Zielinska, and J. E. Wesfreid, "Experimental study of self-sustained oscillations in a confined jet" Phys. Rev. E **54**, 3643–3651 (1996).

[16] Z. Wang, A. C. Bovik, H. R. Sheikh, and E. P. Simoncelli, "Image quality assessment: from error visibility to structural similarity" IEEE T. Image Process. **13**, 600–612 (2004).

[17] http://www.volvis.org